

Magnetostatic interactions on a square lattice

A. Remhof,^{*} A. Schumann, A. Westphalen, and H. Zabel[†]

Institut für Experimentalphysik, Ruhr-Universität Bochum, 44780 Bochum, Germany

N. Mikuszeit and E. Y. Vedmedenko

Institut für Angewandte Physik, Universität Hamburg, Jungiusstrasse 11a, 20355 Hamburg, Germany

T. Last and U. Kunze

Werkstoffe und Nanoelektronik, Ruhr-Universität Bochum, 44780 Bochum, Germany

(Received 7 October 2007; revised manuscript received 13 February 2008; published 3 April 2008)

The metastable zero field magnetic states of elongated Permalloy islands on square lattices of different geometries are investigated by means of magnetic force microscopy and numerical calculations. Keeping the island shape $L/w=10$ fixed while varying the interparticle distances a , it is demonstrated that the relative frequencies of observed magnetic configuration at remanence strongly depend on the packing density of an array and the magnetic history (i.e., in which direction the array has been saturated before measurement). From 16 possible arrangements, only two are experimentally observed. For small L/a , a mixture of configurations, i.e., a spin ice, is found in agreement with previous studies, while for large L/a , an onion state unexpectedly prevails independent of the direction of the previously applied field. The results are discussed within the framework of potential theory and general stray field interaction. The relative frequencies of metastable states as well as the absence of the true ground state are in good agreement with theory.

DOI: [10.1103/PhysRevB.77.134409](https://doi.org/10.1103/PhysRevB.77.134409)

PACS number(s): 75.75.+a, 75.60.Jk, 41.20.Gz

I. INTRODUCTION

Solid state physics deals with the collective behavior of a large number of strongly interacting identical entities. Correlations between the individual constituents may lead to macroscopic order such as the regular arrangements of atoms in crystals or to the long range order of spins in ferromagnetic and antiferromagnetic materials. Artificial patterning opens new opportunities to control and to functionalize the collective behavior of individual micro- and nanometer sized elements. Especially, the technological progress in the field of magnetoelectronics and the advancement in miniaturization techniques brought topological ordered nano- and micro-structured magnetic thin films in the focus of many research activities.¹ One issue is to understand the ground states and magnetization reversal of submicron sized magnetic elements and to functionalize their mutual interactions. Recently, the possibility to build logic devices such as AND and NOR gates on the basis of elongated dipolar coupled Permalloy (Py) has been demonstrated.² In well-ordered artificially structured nanomagnetic dipolar arrays, the interactions arising from stray fields lead to highly correlated systems. In particular, geometric frustration leads to the so-called *spin-ice* state. Spin ice refers to the ice rule, which requires that two hydrogen ions should be close to the oxygen ion and two orthogonal ones further away, forming a distorted tetrahedron.³ This “two in” and “two out” rule can be particularly well applied to magnetic dipole arrays and has recently been investigated by Wang *et al.* in their analysis of a square dipolar pattern.⁴ To realize this state, a two-dimensional square lattice of 25 nm thick Py particles ($80 \times 220 \text{ nm}^2$) was carefully demagnetized and visualized by means of magnetic force microscopy (MFM).⁴

We investigated the remanent state of a Py pattern exhibiting the same symmetry, but with increased length of the

islands and varying gap size between the islands. The frustrated spin-ice state is one of many possible magnetic superstructures that may appear in nanomagnetic arrays. Apart from the shape of the elements, the symmetry of the superstructure depends on the relative distances between the particles. If the interparticle distance a is comparable to or smaller than the length of an element L , higher order magnetostatic contributions become important.⁵ These contributions might induce additional anisotropy and/or select specific vertex configurations from the manifold of the spin-ice symmetries. This, in turn, might influence the magnetization reversal in magnetic arrays. In this study, we experimentally and theoretically investigate the influence of packing density on magnetic structuring in a square array. Theoretically, we find several magnetic superstructures presenting local energy minima. The depth of the minima depends on the geometrical ratio L/a . Experimentally, we investigate the accessibility of these minima in remanence from a saturated magnetic state (sat) with certain orientation of magnetization. In order to obtain the highest possible flexibility in the variation of the geometrical ratio, we use larger Py elements than those used by Wang *et al.*⁴ The magnetic islands, however, still behave as individual entities. Our experiments demonstrate that the remanent configuration depends on the initial orientation of the external magnetic field as well as on the value of L/a . Above a critical geometrical ratio $L/a \geq 3$, several local energy minima are reachable depending on the initial field orientation. For $L/a \leq 3$, a quenching of the degeneracy occurs and the highly ordered onion state is formed in remanence, irrespective of the initial saturation direction. Hence, a fully predictable magnetization state can be achieved.

II. EXPERIMENTAL DETAILS

Starting from closed square frames (or square rings), which have been thoroughly studied in the past,⁶ we discon-

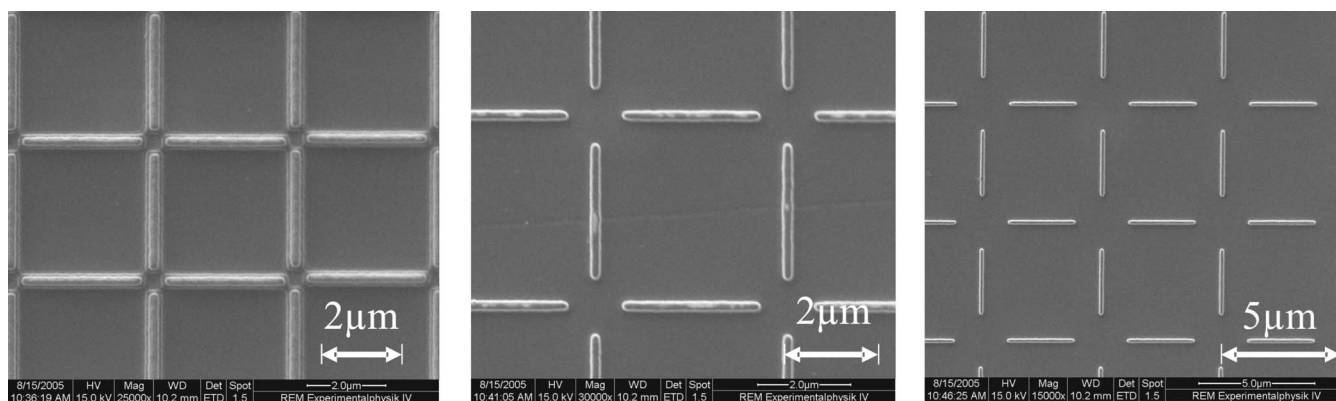


FIG. 1. SEM micrographs of magnetic dipole arrays placed on a square lattice with separation of 0.42, 0.84, and 1.68 μm distances (left to right). Note that the three individual micrographs were recorded with different magnifications; a marker showing the respective length scale has been added to each image.

nected the four equal sides, each one being a rectangular island with a lateral size of $0.3 \times 3 \mu\text{m}^2$. The resulting open frame structure consists of two perpendicularly crossed arrays of islands. To prepare these open frame structures, homogeneous 25 nm thick polycrystalline Permalloy films ($\text{Py}=\text{Ni}_{0.8}\text{Fe}_{0.2}$) were first deposited onto polished Si substrates by ion-beam sputtering. Subsequently, the samples were spin coated with a negative tone resist (ma-N 2403, microresist technologies), and the desired pattern was defined by e-beam lithography using a modified Quanta 200 FEG scanning electron microscope equipped with a Raith Quanta lithography unit. After e-beam exposure and developing, the structures were transferred into the metallic layer by ion beam etching. Several different distances between two adjacent elements were chosen, ranging from 0.4 to 3.6 μm . SEM micrographs of some patterns are shown in Fig. 1. Note that three individual micrographs were recorded with different magnifications; a marker showing the respective length scale has been added to each image.

The aspect ratio and the thickness of the individual Py islands were kept constant and chosen to create single domain particles with high remanence. MFM images of the sample confirm the single domain state of the individual islands in remanence. More patterns can be found in Ref. 7. The MFM images (Nanoscope IIIa, Digital Instruments) were recorded at remanence and at room temperature after saturating the patterns in well defined directions.

III. REMANENT STATES

The open frame system is inherently frustrated. Each vertex where the two sublattices intersect has to accommodate four magnetic poles in close proximity. In the most unfavorable case, four equal magnetic poles meet in a vertex; i.e., the four magnetic moments point all inward or all outward. Energetically, more favorable is a configuration in which two moments point inward and two point outward. Analogous to the steric frustration of hydrogen ions in frozen water, the geometric frustration of spins in a magnetic material has been denoted as spin ice. The spin-ice state is a demagnetized state. It is characterized by a lack of long range order

and by the so-called *ice rules*, which require a minimization of the spin-spin interaction energy when two spins point inward and two spins point outward on each vertex. Model calculations based on the magnetostatic interactions, including multipolar contributions, clearly show that the spin-ice state is, indeed, the demagnetized ground state of the system under investigation.

At remanence, however, the samples exhibit a persistent net magnetization, which is indicative of the existence of a metastable ordered state. The possible symmetric remanent states are shown schematically in Fig. 2. The *onion state*, in which each of the two sublattices is parallelly aligned, has the highest magnetization. The resulting net magnetization of the whole array is tilted by 45° against the long axes of the individual islands. At each vertex, the magnetization of two adjacent elements from different sublattices points inward, while that of the two others points outward.

In the so-called *horseshoe state*, only one of the two sublattices is parallelly aligned, while the other is antiparallelly ordered. Only the parallelly aligned sublattice contributes to the net magnetization, which consequently aligns with the anisotropy axis of the respective islands. There are two possible configurations in the horseshoe state. In the first one, referred to as horseshoe 1 (hs1), at each vertex the magnetization of two adjacent elements from different sublattices points inward, while that of the two others points outward. In the second one, denoted as horseshoe 2 (hs2), at each vertex the magnetization of three elements points inward (or outward), while that of only one points outward (inward). As we will discuss later, we experimentally observe mainly the horseshoe 2 state. In our theoretical calculations to be discussed later, both horseshoe states are taken into account.

The *microvortex state*⁸ exhibits no net magnetic moment. In order to realize the microvortex state, the chirality of two adjacent vortices has to be antiparallel. Also in this state, the magnetization of two elements points inward and that of two points outward. However, opposite to the aforementioned states, this time, the magnetization of two next nearest elements, i.e., from the same sublattice, points inward, while that of the two perpendicular elements from the other sublattice points outward, or vice versa. Consequently, the distance between two equal poles is larger than in the onion or the

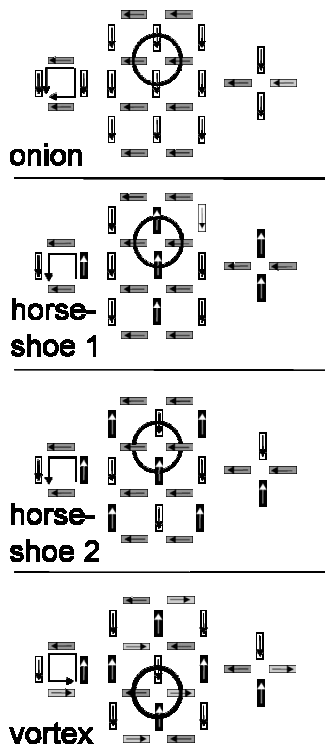


FIG. 2. Schematic representation of the possible symmetrical (meta-) stable remanent states. From top to bottom, the onion state, horseshoes 1 and 2, and the microvortex state are displayed for the crossed structure. The right row depicts a representative square formed of four individual islands, the middle row shows the long range order of the structure, and the left row illustrates a typical vertex of the respective structure. Circles within the extended structure indicate the vertices shown on the right.

horseshoe state, and the distance between two opposite poles is smaller. Thus, this configuration is energetically more favorable than the two arrangements discussed before. The microvortex state can be seen as an “ordered” spin-ice state. It fulfills the condition of demagnetization and the ice rules.

IV. EXPERIMENTAL RESULTS

We have first studied the magnetic state of the open frame structure immediately after growth and without exposure to a magnetic field. In a second set of experiments, the arrays were exposed to a magnetic field up to saturation and then studied by MFM in remanence. We distinguish two possible paths for reaching the remanent state from saturation: In the first one, the field \vec{H} pointed parallel to the diagonal of the frames; i.e., the field makes an angle $\angle(\vec{H}\vec{L})=45^\circ$ with respect to the longest axis of the Py elements \vec{L} . In the second case, the field was applied parallel to \vec{L} , i.e., $\angle(\vec{H}\vec{L})=0^\circ$ for one of the sublattices, which is at the same time perpendicular to the second sublattice.

We first discuss the as prepared state of the open frame structure. In Fig. 3 (a), the MFM images for patterns with distances of $a=0.42, 0.84,$ and $3.4 \mu\text{m}$ are shown. The magnetic poles of the individual islands can be identified by the

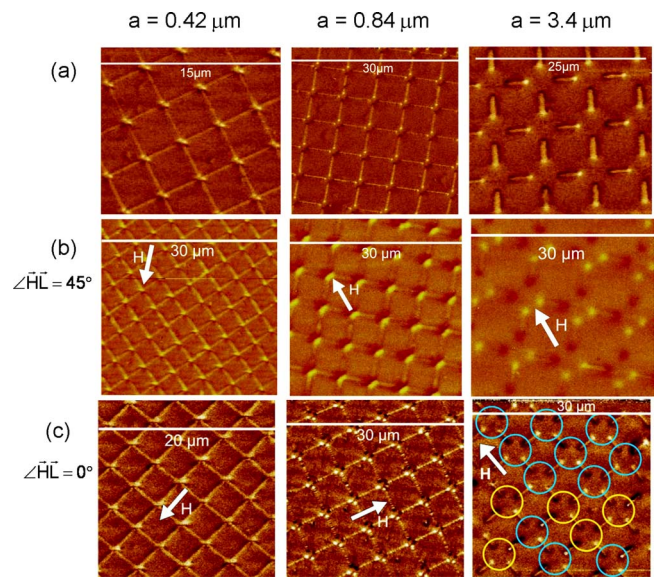


FIG. 3. (Color online) MFM images of Py dipole arrays on a square lattice taken in the remanent state ($H=0$). The individual elements have separations of $0.42, 0.84,$ and $23.4 \mu\text{m}$ (from left to right). (a) shows images in the virgin state of the sample. (b) shows patterns after exposing them to a saturation field applied parallel to the diagonal of the frames (45° state). In (c), the same patterns are shown as in (a) and (b), but with the field applied parallel to one of the sublattices (0° state). The field direction is indicated by white arrows. In the panel to the right, vertices displaying an onion state are highlighted with a blue circle and vertices with a horseshoe state are highlighted with a yellow circle.

black and white spots marking the regions where the stray field leaves and enters the ferromagnetic elements. All vertices show two dipoles in and two out. Furthermore, at each vertex, the magnetization of two adjacent elements points inward, while that of the two others point outward. Thus, we find two ordered sublattices, each one with a collinear magnetization. The superposition gives the perfect onion state. Up to the largest separation investigated ($a=3.4 \mu\text{m}$), no other symmetries are observed. Surprisingly, no vortex states have been observed, although they have a lower energy than the onion state. On the other hand, we cannot completely exclude the possibility that the patterns have been exposed to some stray magnetic field during the sample preparation.

Next, we discuss the $\angle(\vec{H}\vec{L})=45^\circ$ case, which is shown in Fig. 3(b). Saturating along the diagonal axis, the external field has a strong component parallel to the easy axis of all Py particles, resulting in two opposite magnetic poles in a vertex across from each other. We thus expect to find an onion state in remanence, irrespective of the separation of the particles. The MFM images in Fig. 3 confirm this notion for all separations of the particles investigated. In Fig. 3(b), the patterns are essentially identical to the ones shown in Fig. 3(a).

For the $\angle(\vec{H}\vec{L})=0^\circ$ case, the situation is quite different compared to the previous two. Here, the horizontal elements are magnetized parallel to the easy axis, while the vertical elements are magnetized along their hard axis. In remanence, the shape anisotropy of the particles support the magnetiza-

tion along the islands. While it is energetically favorable for the magnetization of the horizontal elements to stay in the field direction, there is no preference for the vertical ones. If the effect of the dipolar interaction of the neighboring elements is negligible (i.e., at sufficiently large distances), 50% of the particles are magnetically oriented north-south, while the other 50% are oriented south-north. Taking dipolar interaction into account, theory predicts for the largest distance the coexistence of the onion state together with the horseshoe 2 state with a ratio of 2:1. This is exactly what we observe. In the right panel of Fig. 3(c), the vortices with an onion state are highlighted with blue circles, the ones with a horseshoe 2 state with yellow circles. The ratio of blue circles to yellow circles is 11:5. This is clearly a limited statistics, but shows the predicted tendency. For smaller distances ($\leq 2 \mu\text{m}$), however, the situation is different. Here, both sublattices are magnetostatically coupled more strongly and simultaneously rotate in the field direction. Then, we expect to observe again the onion state irrespective of the direction the magnetic field is applied to. The MFM images in Fig. 3 confirm this expectation. Indeed, we find solely the onion state at smaller separations. In some perpendicular bars, two domains may be present, as suggested by the central MFM image in Fig. 3(c). However, these do not alter the overall onion state.

Obviously, a deviation from the $\angle(\vec{H}\vec{L})=0^\circ$ case forces the onion state. Experimentally, the critical angle of the transition is not easy to determine. In order to avoid the onion state, the samples have to be aligned very carefully with respect to the applied magnetic field. As the samples can be aligned quite precisely, we conclude that the critical angle lies well below 5° . In OOMMF simulations, any deviation of the field direction forces the sample into the onion state. In real systems, however, roughness and shape irregularities will result in a small but finite value for the critical angle.

V. DISCUSSION

Experimentally, we have shown that the onion state as a remanent state does not only occur in closed frames, as observed by Vavassori *et al.*,⁶ where the four sides forming the structure are in direct contact. Also, open structures, like crossed dipole arrays, exhibiting the same fourfold symmetry possess remanent magnetic states in which the magnetic dipoles are all aligned in one direction for each sublattice as long as the distances between two adjacent elements are small. At larger distances, a frustrated configuration consisting of patches with onion and horseshoe 2 symmetry occurs. Thus, we have demonstrated that the variation in distances between elongated Py elements without any variation of the particle shape changes the remanent configuration of the whole array (see Fig. 4). This means that with increasing interparticle distance, the relative depth of energy minima corresponding to different configurations changes. In the case of one single magnetostatic contribution, e.g., a dipolar one, the absolute depth of energy minima changes with varying a , while the relative energy difference persists. Thus, the change in the relative depth of energy minima can be explained only by a distance dependent cutoff of the higher

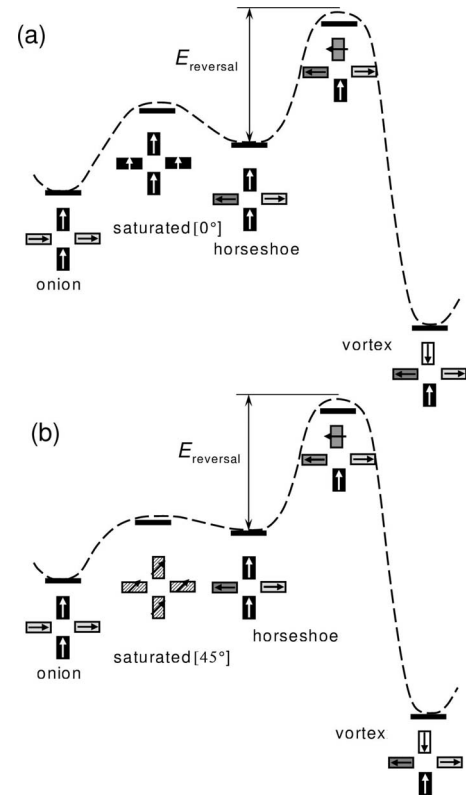


FIG. 4. Schematic representation of the dipole-dipole energy levels of the onion, the horseshoe, the spin ice, and the intermediate states relative to the energy of (a) the 0° saturated and (b) the 45° saturated configurations. The corresponding magnetization configurations are visualized in the insets.

order magnetostatic contributions. Interestingly enough, experimentally obtained magnetic superstructures for both closer and looser packed arrays are different from those reported recently for similar systems.⁴ To analyze the reasons for the unusual structuring, we have theoretically explored the energy landscape and the switching barriers of the Py elements.

In the first set of calculations, the multipole moments of the particles have been determined. As can be expected from previous results,^{5,9} the Py elements have strong odd multipolar contributions Q_{lm} , with l and m independent components of the multipolar tensor Q , i.e., the dipolar Q_{1m} , the octopolar Q_{3m} , and the dotriacontapolar Q_{5m} ones. The strongest octopolar contributions expressed in the strength of the dipolar moment are $Q_{30} \approx 2Q_{10}$ and $Q_{50} \approx 0.5Q_{10}$. The higher order terms are weak $Q_{70} < 0.1Q_{10}$. Hence, for closer packed magnetic arrays, the higher order magnetostatic contributions of at least the third and the fifth order (Q_{3m}, Q_{5m}) have to be taken into account.

To check how the higher order terms influence the magnetic ordering, we have compared pure dipolar $E_{dd}^{\text{configuration}}$ and multipolar $E_{mm}^{\text{configuration}}$ energies of most relevant magnetostatic configurations including the vortex, the onion, and the horseshoe structures and compared them with the energy of the saturated state (see insets in Fig. 4). All of the described configurations have local energy minima in the case of pure dipolar coupling. The depth of an energy minimum is

a relative notion, which is always determined from the comparison of two or several energy levels. In our case, the relevant reference energies are those of the two saturated states described above. In the first one, the magnetization \vec{M} is parallel to the longest axis of a Py element \vec{L} ($\angle \vec{M}\vec{L}=0^\circ$), and in the second case, $\angle \vec{M}\vec{L}=45^\circ$. The corresponding energies are $|E_{dd}^{\text{vortex}} - E_{dd}^{\text{sat}[0^\circ]}| \approx 3 \cdot |E_{dd}^{\text{onion}} - E_{dd}^{\text{sat}[0^\circ]}| \approx 12 \cdot |E_{dd}^{\text{hs2}} - E_{dd}^{\text{sat}[0^\circ]}|$, $|E_{dd}^{\text{vortex}} - E_{dd}^{\text{sat}[45^\circ]}| \approx 5 \cdot |E_{dd}^{\text{onion}} - E_{dd}^{\text{sat}[0^\circ]}|$, and $|E_{dd}^{\text{hs2}} - E_{dd}^{\text{sat}[45^\circ]}| \approx 0$ (see Fig. 4). If the multipolar terms are included, the energy minima for the vortex and the onion configuration decrease further, while the energy of the horseshoe 2 state remains almost unchanged: $|E_{mm}^{\text{vortex}} - E_{mm}^{\text{sat}[0^\circ]}| \approx 5 \cdot |E_{mm}^{\text{onion}} - E_{mm}^{\text{sat}[0^\circ]}| \approx 25 \cdot |E_{mm}^{\text{hs2}} - E_{mm}^{\text{sat}[0^\circ]}|$. Hence, for looser packed arrays where $L/a \leq 3$ (dominating dipolar coupling) as well as for close packed arrays where $L/a \geq 3$ (strong multipole-multipole interactions), the deepest energy minimum belongs to the vortex state. In the following, we analyze energy barriers separating the three local energy minima.

First, we discuss the initial 0° saturation. In the 0° -saturated state, one-half of the Py elements is magnetized along their short axis. This is a hard unfavorable axis from the point of view of the demagnetizing self-energy of a magnet. Therefore, the rotation of the magnetization toward the \vec{L} axis does not cost any energy for these islands. The probability to accept the onion or the horseshoe 2 state is proportional to the depth of the corresponding minimum; i.e., $p_{\text{onion}} \propto \exp[-(\Delta E_{dd/mm}^{\text{onion}})/(kT)]$ and $p_{\text{hs2}} \propto \exp[-(\Delta E_{dd/mm}^{\text{hs2}})/(kT)]$. For looser packed arrays, the dipole-dipole coupling is dominant and $|\Delta E_{dd}^{\text{onion}}| \approx 3.5 \cdot |\Delta E_{dd}^{\text{hs2}}|$. Therefore, the probability to fall into the onion state is approximately 2.5 times larger than that to appear in the horseshoe 2 state. However, $p_{\text{hs2}} \neq 0$, and at least one-third of all transversely magnetized elements should accept this state. This has, indeed, been observed experimentally. In the case of densely packed arrays, the situation changes: the depth of the minimum for the onion state increases ($\Delta E_{mm}^{\text{onion}} \approx 2.25 \cdot \Delta E_{dd}^{\text{onion}}$), while the minimum for the horseshoe state 2 almost disappears $\Delta E_{dd}^{\text{hs2}} \approx 0.5 \cdot \Delta E_{mm}^{\text{hs2}}$. Hence, $|\Delta E_{mm}^{\text{onion}}| \approx 16 \cdot |\Delta E_{mm}^{\text{hs2}}|$ or $p_{\text{hs2}} \rightarrow 0$. Accordingly, no horseshoe 2 state is observed in the experiment.

In the previous paragraph, we have not discussed the microvortex configuration. Although it possesses a global energy minimum, the system has to overcome an energy barrier in order to attain the vortex state. Indeed, one of the initially longitudinally magnetized elements have to be completely reversed (see Fig. 4). Depending on the mechanism (coherent or incoherent magnetization rotation), the magnetization reversal requires an additional energy comparable with that of the magnetostatic coupling. The reversed element should be antiparallel to the applied magnetic field. This makes the magnetization reversal even more energetically expensive. The probability for climbing an energy barrier in the presence of available local minima is close to zero.

Thus, it follows from our calculations that for initial 0° saturation of a Py array, the most probable state is the onion magnetization configuration. However, for large interparticle distances, a relevant number ($\approx 30\%$) of horseshoe 2 states should appear. In remanence, the energetically most favor-

able vortex state is inaccessible because of the large energetic barrier of the magnetization reversal.

A similar analysis has been performed for initially 45° saturated arrays. The corresponding energy landscape is schematically presented in Fig. 4(b). The main difference to the previous discussion is that the total energy of the 45° state is lower than that of the 0° configuration. Therefore, the energy minimum for the horseshoe 2 ordering disappears already for the more widely spaced arrays with dominating dipolar interactions. Hence, if an array has been initially magnetized under 45° to its axes, the onion state should prevail in wider as well in denser packed arrays. An energetically preferred microvortex configuration can be obtained only after a thorough demagnetization of an array.

The last point we would like to theoretically address is the perfect monodomain configuration of all Py elements experimentally found. The size of the islands is much larger than the single domain limit. Therefore, it can be expected that during the magnetization reversal, the magnetic structure of each individual element would accept a complicated multidomain configuration. To find out why this does not happen, we have performed micromagnetic simulations in the framework of the widely used OOMMF package.¹⁰ If the initial orientation of the applied magnetic field has been exactly parallel to the axis of Py elements, we indeed find the multidomain configuration at remanence. However, already for very tiny deviations (less than 1%) between the field and the element's axes, the single domain ordering is restored. These inevitable deviations in real experimental conditions lead to the strict monodomain order in Py dots.

VI. SUMMARY

In summary, we have studied the magnetic ordering of micromagnetic dipole arrays, which are arranged on square lattices. We have taken MFM images of the remanent state either before or after saturating the patterns in a high magnetic field applied parallel to one of the easy axes and along the diagonal of the square pattern. The aim was to investigate the ground states of this inherently frustrated square lattice and to analyze the interplay between external field alignment and internal dipolar stray field depending on the separation of the particles. In detail, we have investigated Permalloy islands with an aspect ratio of about 10 and with variable interparticle distances. Our experiments show that in the virgin state, we observe an onion state independent of the separation of the particles. However, after saturating the patterns in a high field, the remanent configuration depends on the initial orientation of the external magnetic field as well as on the value of L/a . For the smallest interparticle distance of $a \approx 0.4 \mu\text{m}$, we find the onion state prevailing in remanence, independent of the field direction in which the pattern has been saturated. At a separation of $a \approx 3 \mu\text{m}$, both the onion and horseshoe states coexist with a ratio of 2:1, in agreement with theory. The experimental results can be understood on the basis of the magnetostatic energy of the whole system. The energy landscape displays three minima, which can be identified as the microvortex state, the onion state, and the horseshoe 2 state. Therefore, the formation of the microvor-

tex state as the ground state is separated from the observed onion state by a substantial energy barrier. Passing this energy barrier involves the rotation of the magnetization vector of one element through its hard axis configuration. Because of this large energy barrier, the microvortex, although being the ground state, has not been experimentally observed in this work after the saturation of the pattern in high field and the return to remanence.

ACKNOWLEDGMENTS

The authors are grateful for the technical support by Peter Stauche. We would like to thank the DFG for financial support within the framework of the collaborative research centers SFB 491 *Magnetic Heterostructures: Spin Structure and Spin Transport* and SFB 668 *Magnetism From Single Atom to Nanostructure* SFB, projects B3 and A11.

*Also at Eidgenössische Materialprüfungsanstalt, Überlandstrasse 129, 8600 Dübendorf, Switzerland.

†hartmut.zabel@rub.de; URL: <http://www.ep4.ruhr-uni-bochum.de>

¹J. I. Martín, J. Nogues, K. Liu, J. L. Vincent, and I. K. Schuller, *J. Magn. Magn. Mater.* **256**, 449 (2003).

²A. Imre, G. Csaba, L. Ji, A. Orlov, G. H. Bernstein, and W. Porod, *Science* **311**, 205 (2006).

³J. M. Ziman, *Models of Disorder* (Cambridge University Press, Cambridge, England, 1979).

⁴R. F. Wang, C. Nisoli, R. S. Freitas, J. Li, W. McConville, B. J. Cooley, M. S. Lund, N. Samarth, C. Leighton, V. H. Crespi, and P. Schiffer, *Nature (London)* **439**, 303 (2006).

⁵E. Y. Vedmedenko, N. Mikuszeit, H. P. Oepen, and R. Wies-

danger, *Phys. Rev. Lett.* **95**, 207202 (2005).

⁶P. Vavassori, M. Grimsditch, V. Novosad, V. Metlushko, and B. Illic, *Phys. Rev. B* **67**, 134429 (2003).

⁷A. Remhof, A. Schumann, A. Westphalen, T. Last, U. Kunze, and H. Zabel *J. Magn. Magn. Mater.* **310**, 794 (2007).

⁸E. Y. Vedmedenko, *Competing Interactions and Pattern Formation in Nanoworld* (Wiley, Weinheim, 2007).

⁹N. Mikuszeit, E. Y. Vedmedenko, H. P. Oepen, and R. Wiesendanger, *J. Appl. Phys.* **97**, 10J502 (2005).

¹⁰M. J. Donahue and D. G. Porter, OOMMF User's Guide, Version 1.0, National Institute of Standards and Technology Report No. NISTIR 6376, 1999, <http://math.nist.gov/oommf/> (unpublished).